

Suppression and excitation of MHD activity with an electrically polarized electrode at the TCABR tokamak plasma edge

I.C. Nascimento¹, Yu.K. Kuznetsov¹, Z.O. Guimarães-Filho¹,
I. El Chamaa-Neto², O. Usuriaga¹, A.M.M. Fonseca¹,
R.M.O. Galvão^{1,4}, I.L. Caldas¹, J.H.F. Severo¹, I.B. Semenov³,
C. Ribeiro¹, M.V.P. Heller¹, V. Bellintani¹, J.I. Elizondo¹ and
E. Sanada¹

¹ Laboratório de Física de Plasmas, Instituto de Física, Universidade de São Paulo, 05508-090 São Paulo, SP, Brasil

² Universidade Tuiuti do Paraná, 82010-330 Curitiba, PR, Brasil

³ Russian Research Centre, Kurchatov Institute, 123182 Moscow, Russia

⁴ Centro Brasileiro de Pesquisas Físicas, 22290-180 Rio de Janeiro, RS, Brasil

E-mail: inascime@if.usp.br

Received 11 January 2007, accepted for publication 23 August 2007

Published 19 October 2007

Online at stacks.iop.org/NF/47/1570

Abstract

Two reproducible regimes of tokamak operation, with excitation or suppression of MHD activity can be obtained using a voltage-biased electrode inside the edge of the TCABR tokamak. The experiment was carried out adjusting the tokamak parameters to obtain two types of discharges: with strong or weak MHD activity, without biasing in both cases. The plasma current was adjusted to cover a range of safety factor from 2.9 up to 3.5, so that when biasing was applied the magnetic island (3,1) could interact with the edge barrier. The application of biasing in subsequent discharges of each type resulted in excitation or suppression of the MHD activity. The results show that the dominant modes are $m = 2, n = 1$ and $m = 3, n = 1$ for excitation and partial suppression, respectively. In both regimes a strong decrease in the radial electric field is detected with destruction of the transport barrier and of the improved confinement caused by different mechanisms. The measurements include temporal behaviour of edge transport, turbulence, poloidal electric and magnetic fields, edge density, radial electric fields and radial profile of H_α line intensity. The explanation of the excitation and suppression processes is discussed in the paper.

PACS numbers: 52.55.Fa

(Some figures in this article are in colour only in the electronic version)

1. Introduction

Among the main advances in tokamak research are the discovery of the H-mode in ASDEX in 1982 [1] and the realization of the important role played by radial electric fields on plasma confinement, in particular for the control of turbulence. However, the interplay of electric fields and MHD activity has not attracted much attention and, until recently, not very many works have dealt with this issue. In a previous paper we reported the results of the insertion of an electrically polarized electrode at the edge of the tokamak

TCABR showing discharges with increase in the confinement time with small MHD activity, and others with strong MHD and confinement degradation [2]. Recently, similar results have been reported for the TUMAN-3M tokamak [3, 4]. In [5] we investigated the influence of Mirnov oscillations on plasma transport and turbulence in the scrape-off-layer (SOL).

In this work we report recent results of our investigation on MHD activity in experiments with the plasma in confinement regimes similar to the H-mode obtained using a voltage-biased electrode inserted at the edge of the plasma column of the TCABR tokamak. In section 2 we describe the experimental

setup, in section 3 the experimental data are presented and analysed, and in section 4 we present a discussion and conclusion.

2. Experimental setup

The experiments were carried out on the TCABR tokamak, major radius $R = 0.615$ m, minor radius $a = 0.18$ m, toroidal field $B_t = 1.07$ T, maximum plasma current $I_{p,\max} = 110$ kA, circular cross-sectional shape, electron temperature $T_e \sim 500$ eV. In this experimental campaign the density was adjusted at $1.0\text{--}1.5 \times 10^{19} \text{ m}^{-3}$, prior to application of the bias and, depending on the plasma conditions, could grow up to $4.0 \times 10^{19} \text{ m}^{-3}$ with bias, and the plasma current from $I_p = 83\text{--}100$ kA ($q_a = 3.5\text{--}2.9$). The movable electrode is a disc of 20 mm diameter and 8 mm thickness made of hard graphite fixed at the tip of a shaft insulated with an alumina tube. The front face of the electrode can be positioned, without disruptions, up to 2.0 cm into the plasma ($r = 16.0$ cm), at the equatorial plane and low field side of the plasma column, 160° from the graphite limiter in the plasma current direction (counter-clockwise top view). The MHD activity is detected using a set of 22 Mirnov coils, circularly distributed in the poloidal direction at $r = 19.5$ cm (1.5 cm behind the limiter). A set of three Langmuir probes (probe) was used to measure the floating plasma potentials in two poloidal positions separated by 0.5 cm, and the ion saturation current at a toroidal position 0.5 cm apart from the poloidal probes. This triple probe can be moved from $r = 16.0$ cm to 21.0 cm (2.0 inside the plasma to 3.0 cm behind the limiter). In this work the electrode front face position was placed at 17.0 cm or 16.5 cm, depending on the plasma parameters to avoid disruptions, and polarized positively in the voltage range from 300 to 400 V, with respect to the vacuum vessel, which is grounded. The limiter is connected to the vacuum vessel. The ion saturation current and fluctuation potentials, V_{f1} and V_{f2} , at the edge and SOL were measured using a triple probe. Radial profiles were obtained on a shot-to-shot basis. Probe and Mirnov coil data were filtered by a 300 kHz anti-aliasing filter and digitized at 1 megasample per second. The intensity of the H_α hydrogen spectral line was measured using 49 sensors viewing the plasma in the horizontal and vertical directions, for tomography and Abel inversion.

3. Experimental data and analysis

To perform the experiments, the tokamak was configured to obtain discharges with central chord line-averaged densities of $1.0\text{--}1.5 \times 10^{19} \text{ m}^{-3}$ with either strong or weak MHD activity before the application of the bias. The plasma current was programmed to cover a range of safety factors q_a from 3.5 to 2.9, i.e. I_p from 83 to 100 kA, allowing the $q = 3$ rational surface to be placed in the region between the electrode position at 16.5 or 17.0 cm and outside the plasma. The bias voltage duration was chosen to allow a density excursion up to the maximum value.

Two regimes with different effects of electrode bias on MHD activity are shown in figure 1. For regime (a), already shown in our previous work [2], the tokamak was configured to obtain a flat-top plasma current, I_p of 96 kA, ($q_a = 3.0$), up to 70 ms, without electrode biasing. Under these conditions

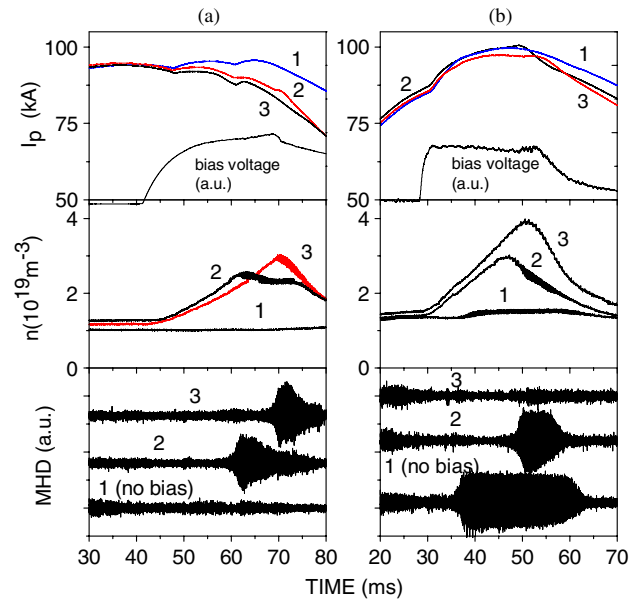


Figure 1. (a) Typical discharges with strong MHD activity during electrode biasing and (b) typical discharges with partial or total suppression of high amplitude MHD activity. Time traces of plasma current I_p , bias voltage V_b , line-averaged plasma density n and MHD activity detected by magnetic probes outside the plasma are shown.

the discharge does not show MHD activity. Subsequently, keeping the same conditions and applying the electrode biasing the discharge shows strong MHD activity with dominant mode $m = 2$, $n = 1$, and the plasma current starts to decrease from flat top even before the onset of the MHD. In regime (b), the plasma current increases with time from 85 kA, $q_a = 3.3$, at 30 ms, reaches a peak of 100 kA, $q_a = 2.9$, around 40 ms, and decays after 50 ms. Without or with electrode biasing the change of plasma current is less than 3%. We have chosen this regime for studies of plasma biasing because it shows quite different behaviour as compared with regime (a), i.e. reproducible excitation of strong MHD activity with dominant mode $m = 3$, $n = 1$ without bias and total or partial suppression of MHD when the bias is applied before the MHD burst, at about 30 ms.

We observe various effects of plasma biasing at close experimental conditions, as can be seen in figure 1–3. There can be total MHD suppression (shot 18699), small bursts of MHD during biasing and large bursts after biasing (shot 18722), or during biasing (shot 18691). The last case was the most reproducible, with high enough bias voltage/current, in both regimes (shot 2 in figure 1, shot 18691 in figure 2 and shots 17994, 18696 in figure 3). Electrode biasing applied during MHD burst in regime (b) did not produce suppression, and the increase in plasma density is very weak, as can be seen in figure 2, shot 18077. The interesting regimes of the shots 18699 and 18077 were not yet studied in the TCABR tokamak.

Tests made with gas puffing to obtain similar temporal evolution of the plasma density as that with biased electrode did not show equivalent results [2]. Therefore, we concluded that the effects described in this paper are caused by the influence of a transport barrier created by the electrode voltage.

The time behaviour of important parameters of the well-reproducible discharges 17994 and 18696, regimes (a) and (b),

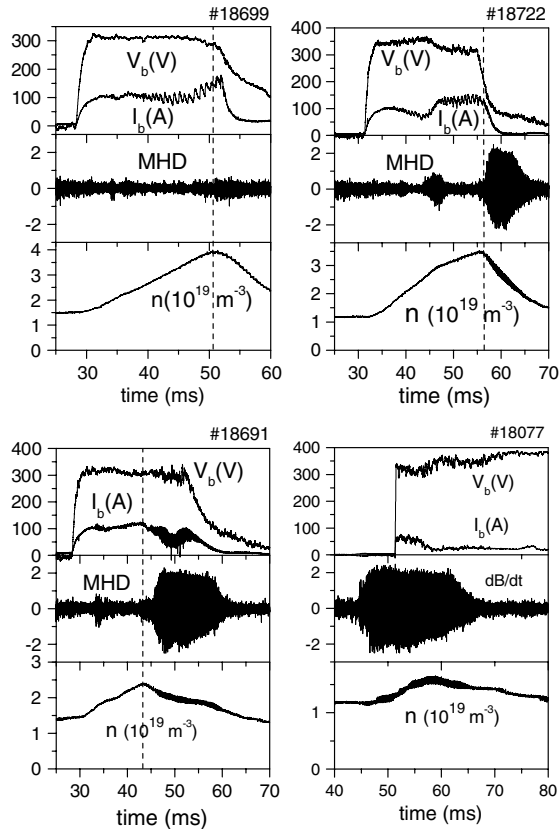


Figure 2. Various effects of plasma biasing in the regime of MHD suppression: total suppression of MHD (shot 18699), partial suppression with small burst of MHD during biasing and MHD excitation after biasing (shot 18722), partial suppression with large burst of MHD during biasing (shot 18691). There is no suppression in the case of plasma biasing applied during the MHD burst, and the effect of biasing on plasma particle confinement is small in this case (shot 18077).

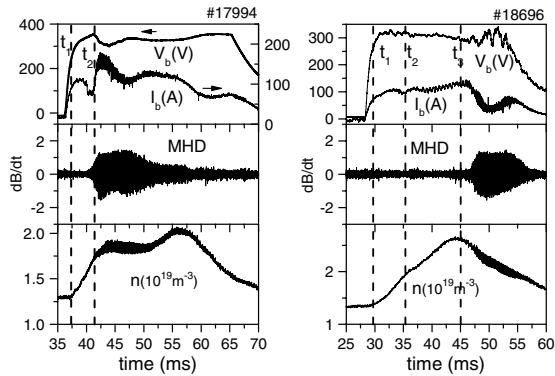


Figure 3. Regimes of MHD excitation, regime (a) (shot 17994) and partial suppression, regime (b) (shot 18696) with electrode biasing. Time traces of bias voltage V_b and current I_b , burst of MHD activity detected by magnetic probes outside the plasma, and central chord line-averaged plasma density n , measured by microwave interferometer, are shown. In the regime of shot 18696, the MHD activity is excited without bias in the time interval 37–63 ms similarly to shot 1 of figure 1.

respectively, is presented in figures 3 and 4. The triple probe was located at $r = 17.0$ cm, i.e. 1.0 cm inside the plasma in the region of the transport barrier and the electrode at $r = 16.5$ cm for shot 17994 and 17.0 cm for shot 18696.

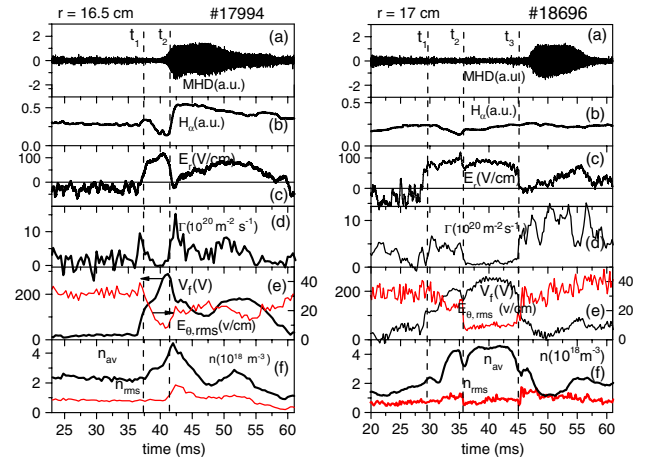


Figure 4. Effect of electrode biasing on edge plasma parameters. Regimes of MHD excitation (shot 17994, electrode position $r = 16.5$ cm) and suppression (shot 18696, electrode position $r = 17$ cm). (a) Signal of magnetic probe located outside the plasma, (b) H_α emission at the electrode, (c) radial electric field measured on shot-to-shot basis for shots 17994/17993 and 18696/18695, (d) turbulent particle transport obtained from measured potentials and ion saturation current, (e) floating potential and rms amplitude of poloidal electric field and (f) time averaged local plasma density and rms amplitude of its oscillations.

The average radial electric field shown in figure 4 was obtained by taking the gradient of the floating potentials measured by the 3-pin Langmuir probe at positions 17 and 18 cm in two successive shots (shots 17993/17994 and 18695/18696), with good reproducibility. The temperature was not measured concomitantly and this correction was not included in figure 4. Measurements made in similar conditions indicated that it can amount to about 20–30% in the region of interest. However, since this correction is always in the direction of increasing the electric radial field it does not influence the conclusions of this work. The turbulence-induced flux Γ shown in figure 4 was calculated with averaging on rather short time intervals, for better temporal resolution: 0.4 ms in 17994 and 1 ms in 18696. This fact explains rather large low-frequency random oscillations in Γ .

In the regime of bias excited MHD activity, shot 17994, the average plasma density, measured at the central chord by the microwave interferometer, increases (figure 3), while the H_α emission decreases (figure 4), indicating improved global particle confinement. The edge transport barrier formation in the time interval t_1 – t_2 is inferred from the increase in radial electric field to positive values ~ 100 V cm $^{-1}$, concomitant with increase in local plasma density at the edge and decrease in local density at the SOL [2] (not shown here), indicating steepening of the density profile at the edge. The decrease in the poloidal electric field and plasma density oscillations results in a decrease in the turbulence-driven particle transport $\Gamma = \langle \tilde{n}_e \tilde{v}_r \rangle$. At the onset of MHD activity, the deterioration of the barrier is apparent, indicated by the increase in the H_α emission and turbulent transport, the decrease in the radial electric field and local density, and the stop in the increase in the central chord line-averaged density. Later, as the MHD activity decreases, the density increases again, reaching a peak, showing again particle confinement improvement.

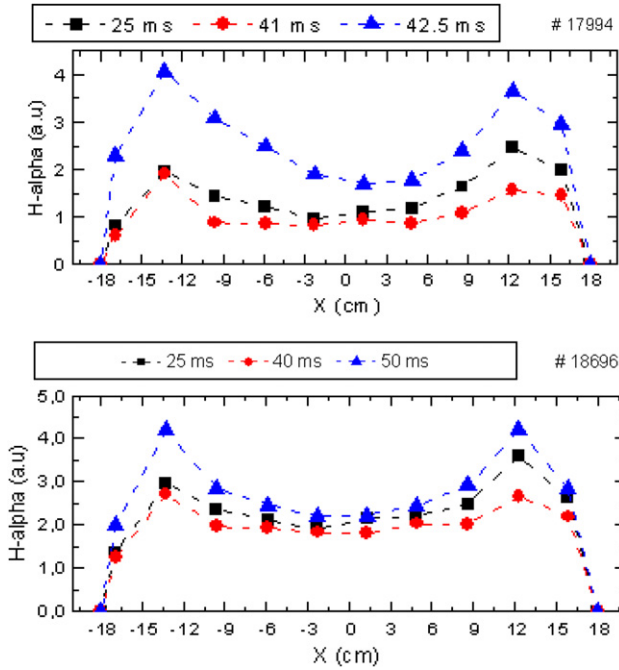


Figure 5. Radial profiles of the H_α emission before biasing (■), with biasing before the burst of MHD activity (●), and with MHD activity (▲).

These results lead to the conclusion that plasma turbulence is suppressed by electrode bias, but increases again with the growth of MHD oscillations.

In the regime of bias suppressed MHD activity, shot 18696, the plasma density grows gradually during the time interval t_1-t_3 (figure 3). There is a strong and reproducible event during time interval t_2-t_3 , (figure 4, from 35 to 45 ms), similar to an L–H transition (bifurcation) observed in other experiments on bias electrode [6–8], namely, a sudden drop in plasma turbulence and related transport. However, in contrast to [6–8], we do not observe a strong correlated drop in electrode current and increase in the rate of plasma density rising. The H_α (not normalized) spectral line intensity increases slightly, but the radial profile shows a decrease everywhere, as can be seen in figure 5, comparing values before, during and after the event. In contrast to the case of shot 17994, here the radial electric field E_r , average plasma density, and local density at the edge start to decrease 2–4 ms before the rapid growth of the MHD activity. We would also like to point out the quite different behaviour of the electrode current and H_α emission in these two regimes. In the case of shot 17994, MHD activity leads to a strong increase in the electrode current and H_α emission, while in shot 18696 the electrode current decreases and H_α emission remains about the same. We conclude that together with the common main features of these two regimes, namely, formation of the ETB by plasma biasing and its destruction by a high level of MHD activity, there can be many differences in the detailed behaviour of plasma parameters.

In both regimes shown in figures 3 and 4 the average radial electric fields show strong drops, and then recover slowly while the MHD amplitude is still high. However, this increase in E_r does not provide the recovery of the ETB as expected. The average plasma density does not increase in shot 17994 until decay of the MHD activity and, on the other hand, the

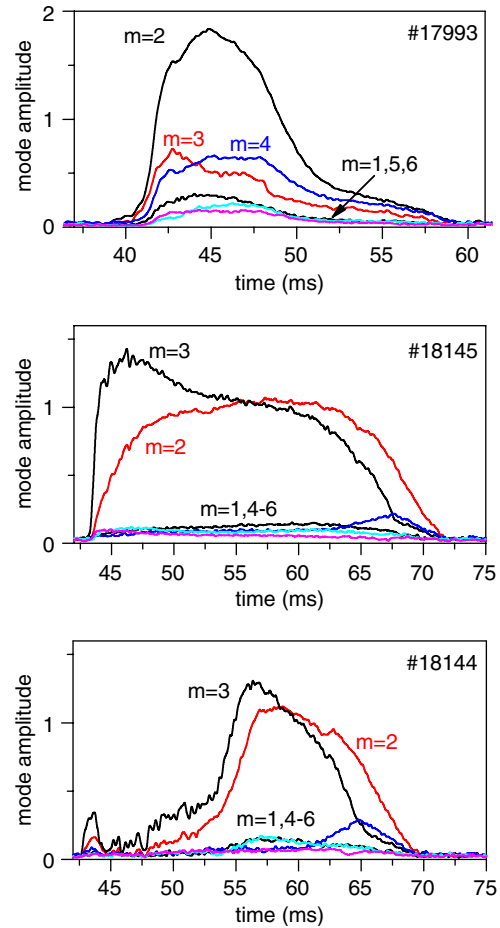


Figure 6. Time behaviour of MHD poloidal modes $m = 1-6$. In shot 17993, the MHD activity is absent without bias and it is excited with bias. In shot 18145, the MHD activity is excited without bias, and its partial suppression occurs with bias (shot 18144). It can be seen that mode $m = 2$ is dominant in shot 17993 and mode $m = 3$ is dominant in shot 18145 at the beginning of the MHD activity. In shot 18144 modes $m = 2, 3$ have close amplitudes.

density in shot 18696 is already decreasing at the onset of the MHD activity. In both regimes the local density at the edge shows some correlated but rather weak recuperation. The local turbulent transport does not decrease in response to the recovery of E_r , presumably because the electric field gradient, directly responsible for the ETB, remains small due to the high level of MHD activity.

The temporal evolution of the MHD mode spectra is presented in figure 6 for the two regimes. For excitation it is presented for shot 17993, which has the same characteristics of the shot 17994. For shot 18696, we present instead data for similar shots of this regime, 18144 and 18145 because some magnetic probes were damaged. In the case of excitation the dominant mode is (2,1), and mode (3,1) is substantially less intense. Without bias (shot 18145), the burst of MHD activity starts with dominant mode $m = 3$, and mode $m = 2$ grows with time. With bias (shot 18144), partial suppression of MHD is observed, with comparable amplitudes of modes $m = 2, 3$.

It is observed (figures 1 and 7) that mode (3,1) is excited without biasing in the regime (b), while MHD activity is absent at close values of plasma current in regime (a). A possible

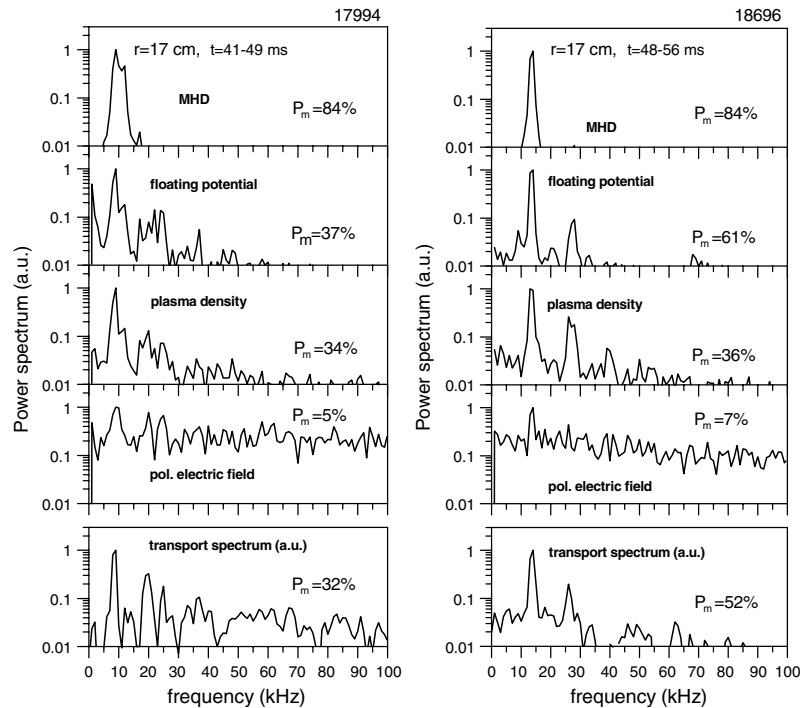


Figure 7. Power spectra of MHD oscillations, floating potential, plasma density (ion saturation current) and poloidal electric field. Particle transport spectrum is shown in the bottom part of the figure. Here P_m is calculated as part of total power related to the frequency interval of MHD activity, 7–10 kHz for shot 17994 and 12–15 kHz for shot 18696.

explanation for the excitation of the edge mode (3,1) in the regime (b) is that the plasma current is increasing with time modifying the current density gradient at the plasma edge, due to the skin effect. It is also possible that impurities contribute to this different behaviour.

The power spectrum of MHD oscillations measured outside the plasma by magnetic probes shows dominant frequency of 8–14 kHz (figure 7). The floating potential and plasma density at the plasma edge, measured with triple probe, are strongly modulated by the MHD frequency. The poloidal electric field has substantially lower modulation. However, the particle transport spectrum shows rather high transport in the frequency interval of MHD activity, 32% of total particle flux in shot 17994 ($f = 7$ –10 kHz) and 52% in shot 18696 ($f = 12$ –15 kHz).

The power spectra presented in figure 7 were calculated averaging on the full time interval of the MHD bursts. In fact, these spectra are not stationary, as can be seen in figure 8 where the temporal evolution of particle transport is presented. As can be seen, bursts of turbulent particle flux can occur with twice the MHD frequency and simultaneous decrease of transport on the fundamental frequency. In some time intervals there are no peaks of transport on MHD frequencies. We can also see that destruction of transport barrier in shot 18696 before strong MHD activity, discussed above (figure 4), can be explained in figure 8 ($t = 44$ –46 ms) by a strong increase of transport at very low frequencies, $f = 1$ –3 kHz.

4. Discussion and conclusion

Transport barrier destruction with MHD activity excitation observed in the present experiment agrees qualitatively with

expectations. Magnetic perturbations lead to a decrease in the radial electric field due to the decrease in plasma resistivity for radial plasma current, and have strong negative effect on confinement when the magnetic island (3,1) overlaps with the region of the edge transport barrier. Experimental data of shot 17994 confirm this model. The radial electric field always drops and plasma turbulence increases with the burst of MHD activity (figure 4), and plasma parameters are strongly modulated by the MHD frequency (figure 7).

From the E_r decrease and the increase in turbulence-induced flux $\Gamma \sim 2$ ms before MHD in the regime (b) shot, 18696, (figures 3, 4 and 8), one can infer that the recuperation of MHD and destruction of the ETB are caused, initially, by the low-frequency instability, $f \sim 1$ –3 kHz, clearly seen in figure 8. This short-time instability is strong enough for destruction of the ETB but then it is replaced by the MHD activity, which maintains the destruction.

Let us discuss the observed excitation or suppression of MHD by bias electrode depending on the regime of tokamak operation. We consider that differences in the MHD mode structure play an important role in the present situation.

The instable modes (2,1) and (3,1) are often observed in tokamaks with q_a close to 3 and are predicted by theory. In general the plasma biasing leads to strong changes of the plasma profiles and excitation or suppression of MHD by biasing can be expected.

In regime (a) of bias excited MHD, the mode (2,1) is dominant (figure 6, shot 17993). The mode (3,1) has substantially lower amplitude and is probably caused by toroidal coupling. This excitation of MHD activity is possible due to changes of radial plasma profiles, produced by accumulation of impurities in the central region of the plasma

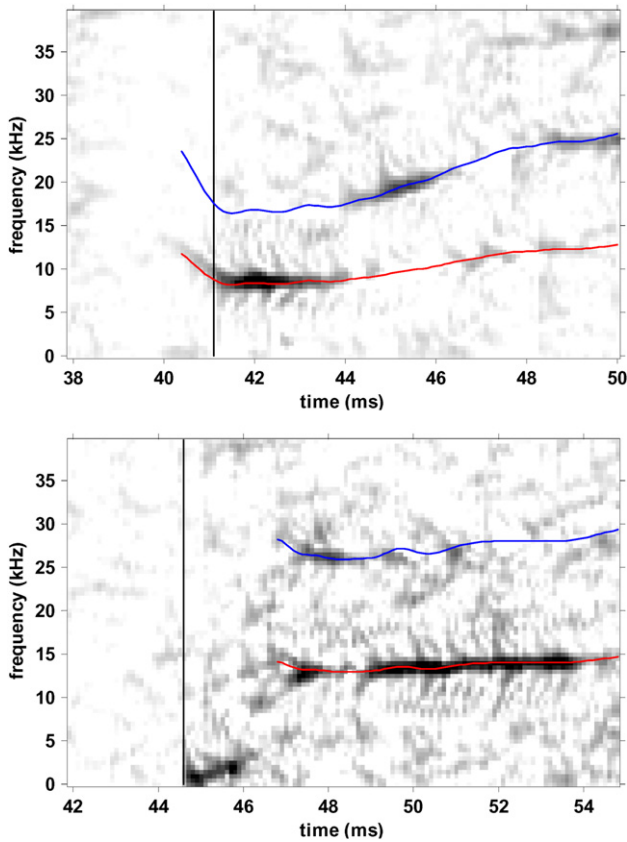


Figure 8. Temporal evolution of particle transport with excitation of MHD activity. Main MHD frequency and its double frequency are shown by the lines.

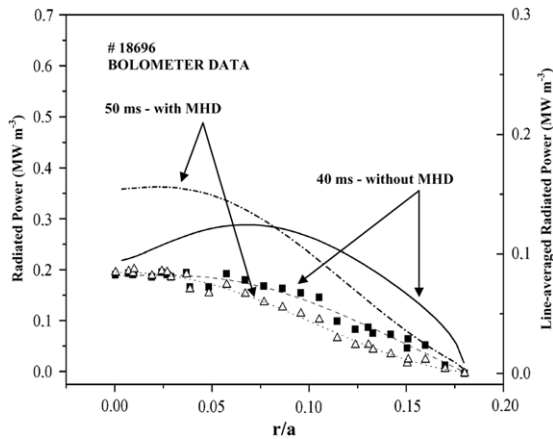


Figure 9. Radial profile of the radiated power obtained with bolometer array for discharge 18696. Experimental data are identified by different symbols: squares for radiation emitted during improved confinement and triangles during the MHD burst. Lines represent reconstructed radial profiles of line-averaged radiated power and local power.

column, similarly as indicated by bolometric measurements shown in figure 9 for shot 18696. The onset of the MHD activity and the overlapping of the magnetic islands (2,1) and (3,1) lead to magnetic stochasticity of the edge barrier region producing a fast decrease in the electric field and destroying the edge barrier. This interpretation is in qualitative agreement with Stringer's neoclassical theory of impurity transport in

the presence of electrostatic and magnetic fluctuations [9]. The density comes back to increase with the decrease in the amplitude of the MHD islands.

In regime (b) of partially suppressed MHD with biasing (figure 6, shot 18696) the breakdown of the transport barrier seems to be a consequence of the low-frequency (1–3 kHz) strong mode in figure 8, which shows the particle transport as a function of time. It can be seen that it starts 0.5 ms before the fast decrease in E_r and is followed by the growth of the large islands (3,1) and (2,1), both rising gradually (figure 6, shot 18145) and reaching comparable amplitudes. Figure 9 shows that the peak of the radiation profile, measured using a bolometer array and Abel inversion, is close to the plasma centre, indicating concentration of impurities and larger emission of radiation. Also in this shot the position of the electrode at $r = 17.0$ cm makes the electrode current very sensitive to small changes in the plasma position, which can explain the decrease in the bias current. The origin of the precursor instability of (1–3) kHz is a problem for future investigation.

In conclusion, using voltage polarized electrodes inserted into the edge of the TCABR tokamak to study confinement improvement two regimes of operation were obtained and studied: excitation and partial suppression of high-level MHD. The important results are given in the sequence.

- For the regime of excitation of MHD activity with electrode biasing, a transport barrier of short duration is created but with the increase in the particle confinement time, impurities accumulate in the central region of the plasma column and cause the excitation and growth of magnetic islands, leading to a strong decrease in the electric field and consequent destruction of the ETB. Therefore, this can be considered a secondary effect of the barrier dependence on the plasma conditions.
- In the regime of suppression of MHD, the application of the bias produces a strong improvement of the particle confinement and the ETB changes the plasma parameters in the plasma edge inhibiting the (3,1) and (2,1) MHD modes. It is expected that sheared plasma rotation contributes to the suppression. However, in the particle transport, a mode with frequency changing from 1 to 3 kHz is detected in coincidence with a strong decrease in the radial electric field, increase in turbulence and H_α intensity, and consequently destruction of the ETB. As soon as this mode dies out, the MHD activity at the usual higher frequency is restored. Accumulation of impurities in the central region of the plasma is detected using a bolometer array and Abel inversion of bolometric measurements. Here the suppression is the main effect and the restoring of the MHD is a secondary effect dependent on the plasma conditions.

Acknowledgments

This work was supported by the FAPESP—Research Foundation for the Support of the Research of the State of Sao Paulo, CNPQ—National Council of Scientific and Technological Development, University of Sao Paulo, and IAEA-CRP-Joint Research using small tokamaks.

References

- [1] Wagner F. *et al* 1982 *Phys. Rev. Lett.* **49** 1408
- [2] Nascimento I.C. *et al* 2005 *Nucl. Fusion* **45** 796
- [3] Askinazi L.G. *et al* 2006 *Plasma Phys. Control. Fusion* **48** A85
- [4] Bulanin V.V. *et al* 2006 *Plasma Phys. Control. Fusion* **48** A101
- [5] Heller M.V.A.P *et al* 2005 *Czech. J. Phys.* **55** 265
- [6] Taylor R.J. *et al* 1989 *Phys. Rev. Lett.* **63** 2365
- [7] Boedo J. *et al* 2000 *Nucl. Fusion* **40** 1397
- [8] Weynants R. *et al* 1992 *Nucl. Fusion* **32** 837
- [9] Stringer T.E. 1992 *Nucl. Fusion* **32** 1421